Macromolecules

ARTICLE

pubs.acs.org/Macromolecules

Functionalization of Titanium Surfaces with Polymer Brushes Prepared from a Biomimetic RAFT Agent

Cédric Zobrist,[†,‡,§] Jonathan Sobocinski,[†,‡,§] Joël Lyskawa,[†,‡,§] David Fournier,[†,‡] Valérie Miri,[†,‡] Michel Traisnel,[†,‡,§,⊥] Maude Jimenez,[†,‡,§,⊥] and Patrice Woisel[†,‡,§,⊥,*]

[†]Université Lille Nord de France, F-59000 Lille, France

[‡]USTL, Unité des Matériaux Et Transformations (UMET, UMR 8207), Equipe Ingénierie des Systèmes polymères (ISP), F-59655 Villeneuve d'Ascq Cedex, France

[§]Fédération Biomatériaux et Dispositifs Médicaux Fonctionnalisés (BDMF/FED 4123), F-59655 Villeneuve d'Ascq, France

[⊥]ENSCL, F-59655 Villeneuve d'Ascq, France

Supporting Information

ABSTRACT: Well-defined dopamine end-functionalized polymers were synthesized by employing the reversible addition−fragmentation chain transfer (RAFT) polymerization technique. *tert*-Butyl acrylate, *N*-isopropylacrylamide, and styrene monomers were polymerized in the presence of azobis (isobutyronitrile) and a new catechol-based biomimetic RAFT agent incorporating a trithiocarbonate unit. All RAFT polymerizations exhibited pseudofirst-order kinetics, a linear increase of the number-average molar mass (M_n SEC) with conversion and narrow molar mass distributions (polydispersity <1.2). The resulting homopolymers exhibited the electroactive catechol and the ω-trithiocarbonyl end groups. Subsequent immobilization of dopamine end-functionalized polymers on titanium surfaces was monitored by using a surface plasmon resonance (SPR) sensor, and the resulting films were characterized by contact angle, infrared ATR spectroscopy, atomic force microscopy (AFM), and X-ray photoelectron spectroscopy (XPS).

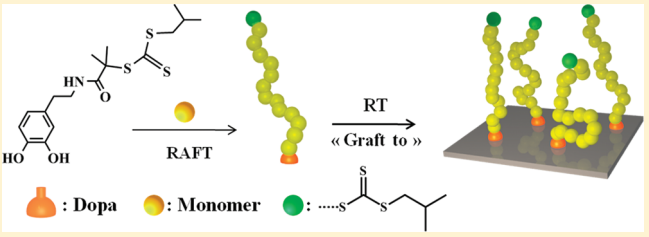

INTRODUCTION

Titanium and its alloys are attractive materials due to their unique biocompatible,[1] mechanical,[2] thermal,[3] and electrical[4] properties. These properties make them useful in a wide range of structural, chemical, nanotechnological, and biomaterial applications. Controlling the functionality of exposed titanium surfaces is of great importance for improving their performance (and thus also for their practical applications). Titanium-based orthopedic implants and nanoparticules, for example, often require chemical modification of the surface for controlling specific cell adhesion[5] and to avoid the aggregation of the TiO_2 nanoparticles,[6,7] respectively. Hence, over the last two decades, considerable efforts have been devoted to engineering the properties of the titanium surface through the development of efficient methods allowing the manipulation of the surface's chemical composition and topology.[8−10]

Tethering of polymer brushes to a surface[11] has emerged as promising tool to tailor surface properties such as wettability, corrosion resistance and adhesion for applications including microelectronics,[4] biomedical devices,[12,13] nanopatterning,[14] and thermoresponsive adhesives.[15,16] Polymer brushes can be immobilized on appropriate surfaces using either a physisorption (i.e., chain attachment mainly through van der Waals interactions) or a covalent (i.e., anchoring by chemical bonds) strategy. The main disadvantages of the physisorption of polymers are the relatively thermal and solvolytic instabilities due to the noncovalent grafting. Alternatively, several techniques for covalently tethering well-defined polymer brushes onto surfaces have been developed, including the covalent attachment of end-functionalized polymers incorporating an appropriate anchor ("grafting to") and the *in situ* polymerization initiated from the surface ("grafting from").[17] While the "grafting from" strategy generally leads to higher grafting surface densities, the "grafting to" approach, thanks to the known structures and the easy processability of the linear brush precursors, offers the unique opportunity to easily tune the surface properties.

Typically, the attachment of well-defined polymer brushes to a titanium surface was achieved by using either the "graft from" or the "graft to" approaches, and by mostly applying living polymerization techniques including opening metathesis[18] and living radical polymerizations (LRP).[6,19,20] Of these living radical polymerization techniques, atom transfer radical polymerization (ATRP)[21] has been the most widely employed.[19,20,22] Nevertheless, reversible addition−fragmentation chain transfer (RAFT) polymerization presents some advantages over ATRP polymerization. Both techniques allow the polymerization of a

Received: April 13, 2011
Revised: July 1, 2011
Published: July 14, 2011

large array of monomers, including (bio)functional monomers,[23] under a variety of reaction conditions; however, the RAFT process does not require the use of a toxic metal (i.e., copper) catalyst. Moreover, recent cytotoxic results regarding polymers prepared by a RAFT procedure have shown that polymers elaborated from a trithiocarbonate RAFT agent did not affect either the morphology or the viability of different adherent cell lines (CHO-K1, RAW264,7, NIH3T3).[24] Surprisingly, few research works were reported in the literature to tether brush polymers onto a titanium surface by using a RAFT procedure. These mostly concern the grafting of well-defined PMMA polymers onto Nano-TiO_2 using a carboxylic acid group as anchor in a view to overcome the self-aggregation of nanoparticules.[25] However, carboxylate-type anchors usually exhibited weak and unstable bindings with a titanium surface, in particular in aqueous environments that notably limit their exploitation for the development of functionalized materials in contact with biological media. Therefore, a grafting strategy allowing the immobilization, through a more robust binding mode, of well-defined polymer brushes prepared by RAFT procedure would seem to be largely superior.

Recently, the catechol unit has emerged as a very promising ligand for the functionalization of a wide range of substrates including polymers, semiconductors, and more importantly, metals and metal oxides.[26−30] In particular, biomimetic dopamine has sparked great interest as an anchor for the functionalization of metal oxide surfaces due to the stability and strength of the resultant five-membered metallocycle chelate and the ability of this anchor to be chemically modified through amide bonds.[31−33] Hence, the ability of dopamine derivatives to strongly bind titanium oxide surfaces has been exploited to immobilize brush polymers onto titanium surfaces from end-functionalized dopamine PEG[28,34,35] or by using living polymerization techniques such as ring-opening metathesis polymerization (ROMP)[18] or ATRP.[22,26,29,36]

Here, we report the use of the RAFT procedure to produce various well-defined dopamine end-functionalized polymers and their subsequent and direct immobilization on a titanium surface. To achieve this goal, we have designed and synthesized a new trithiocarbonate type RAFT agent incorporating an electroactive dopamine moiety, which was used to mediate RAFT polymerizations of common monomers such as *tert*-butyl acrylate, *N*-isopropylacrylamide, and styrene under conditions that provide kinetic and molar mass control. Subsequent immobilization of polymers on the titanium surface was monitored by using a surface plasmon resonance (SPR) sensor, and the resulting films were characterized by contact angle, atomic force microscopy (AFM) and X-ray photoelectron spectroscopy (XPS) investigations.

EXPERIMENTAL SECTION

Materials. All reagents were purchased from Sigma-Aldrich and used without further purification unless otherwise noted. *t*-Butyl acrylate (>99%, Acros Organics) and styrene (99%, Aldrich) were purified by vacuum distillation under reduced pressure before use. *N*-Isopropylacrylamide (NIPAM, 99% Acros Organics) was recrystallized from hexane. The primary radical source used in all polymerizations was azobis (isobutyronitrile) (AIBN, >98%, Fluka) and was used as received. The 2-(1-isobutyl) sulfanylthiocarbonylsulfanyl-2-methylpropionic acid (CTA) was synthesized as previously described.[37] All polymerizations were conducted in a nitrogen atmosphere.

Analytical Techniques. ^{1}H NMR spectra were recorded at 25 °C, with a Bruker Avance 300 spectrometer. The number-average molar mass (M_n), the weight-average molar mass (M_w), and the molar mass distributions (M_w/M_n) were determined by size exclusion chromatography (SEC) in tetrahydrofuran at 40 °C with a flow rate of 1 mL.min^{-1}. The number-average molar masses (M_n), the weight-average molar masses (M_w), and the polydispersity indices (PDI = M_w/M_n), were derived from the refractive index (RI) signal by a calibration curve based on polystyrene (PS) standards from Polymer Standards Service. In all plots showing the evolution of M_n with monomer conversion, the straight line corresponds to the expected evolution of the theoretical number-average molar mass, $M_{n,th}$ defined as $M_{n,th}$ = ([Monomer]/[CTA]) × conversion + M_{CTA}.

A Varian Cary 50 Scan UV/vis spectrophotometer was used for UV studies. All electrochemical experiments (cyclic voltammetry) were performed using an Autolab PGSTAT 30 workstation. The electrolyte solution (0.05 M) was prepared from recrystallized tetrabutylammonium hexafluorophosphate (Bu_4NPF_6) and dry acetonitrile or dry dichloromethane. A three-electrode configuration was used with a platinum disk (2 mm diameter) as working electrode, with an Ag/AgCl reference electrode and a platinum wire as the counter electrode. All measurements were recorded at 20 °C under a nitrogen atmosphere. The solution was purged with nitrogen prior to electrochemical analyses.

Surface Plasmon Resonance (SPR) measurements were carried out with a mono channel, AutoLab Springle instrument (Eco Chemie, The Netherlands). Briefly, polarized laser light (l = 670 nm) is directed to the bottom side of the titanium disk (diameter =2.54 cm) sensor via a hemispheric lens placed on a prism (BK7 having a refractive index of n = 1.52) and the reflected light is detected using a photodiode. An autosampler (Eco Chemie, The Netherlands) is used to inject or remove the tested solutions. All SPR measurements were done in nonflowing liquid conditions, i.e. with the circulating pump paused, and at 20 °C. The noise level of the SPR angle is ∼1 m degree. After each addition, the cell was thoroughly washed with the used solvent. All measurements were conducted at 20 °C. The substrates were allowed to equilibrate until a steady baseline was observed.

XPS analyses were performed on a Kratos Axis Ultra DLD system (Kratos Analytical) using a monochromatic Al Kα X-ray source ($h\nu$ = 1486.6 eV). The emission voltage and the current of this source were set to 15 kV and 10 mA, respectively. The pressure in the analyzing chamber was maintained at 10^{-9} mbar or lower during analysis, and the size of the analyzed spot is 500 μm. Survey (0−1200 eV) and high resolution (C 1s) spectra were recorded at a pass energy of 160 and 40 eV, respectively. XPS analyses were performed with a takeoff angle of 90° relative to the sample surface. The core level spectra were referenced with the Ti 2p binding energy at 458.7 eV. Data treatment and peak-fitting procedures were performed using Casa XPS software.

IR-ATR spectra were recorded on a Spectrum One spectrometer from Perkin-Elmer coupled with a Zn/Se ATR crystal collecting 64 sample scans.

Contact angle measurements were evaluated with a Digidrop contact Angle Meter from GBX Scientific Instruments at room temperature. A water drop was used to measure contact angle values (θ). The measurement was repeated five times to obtain an average value for the surface.

Atomic force microscopy (AFM) experiments were carried out in air, at room temperature, in a Nanoscope III multimode microscope from Digital Instruments, operating in tapping mode. The experimental set up consists of integrated silicon tips with a radius of curvature of about 2 nm, and cantilevers (model SSS) with a free oscillation frequency f_0 of ca. 160 kHz. For all experiments, driving oscillation frequency was 250 Hz lower than f_0. Images were recorded by maintaining a set point ratio r_{sp}. (ratio of the magnitude of the engaged amplitude to the free air

Scheme 1. Synthesis of Dopa-CTA and the Resulting Dopamine End-Functionalized Polymers

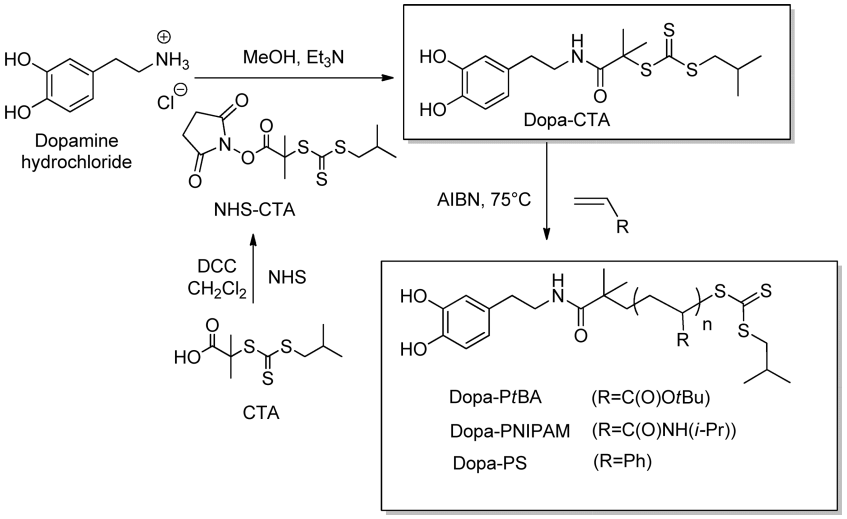

amplitude of the oscillating silicon tip) of 0.90, using a scanning frequency of 0.3 Hz.

Synthesis of the Succinimide-Based Chain Transfer Agent (Suc-CTA). A suspension of *N*-hydroxysuccinimide (NHS, 3.3 g, 29.7 mmol) in dry dichloromethane (100 mL) was added dropwise, at −10 °C and in a nitrogen atmosphere, to a solution containing 2-(1-isobutyl)sulfanylthiocarbonylsulfanyl-2-methylpropionic acid (CTA, 5.0 g, 19.8 mmol) and dicyclohexylcarbodiimide (DCC, 6.5 g, 29.7 mmol) in dichloromethane (150 mL). The mixture was allowed to stir overnight at room temperature. The solvent was evaporated, leaving a crude product which was then subjected to column chromatography (SiO_2: ethyl acetate/petroleum ether 3:1). The product was obtained as a bright yellow solid in a quantitative yield.

^{1}H NMR (300 MHz, $CDCl_3$), δ (ppm from TMS): 0.94 (d, J = 6.7 Hz, 6H, CH-(CH_3)$_2$), 1.80 (s, 6H, C(CH_3)$_2$), 1.92 (m, 1H, CH_2−CH-(CH_3)$_2$), 2.75 (s, 4H, (C═O)−CH_2−CH_2−(C═O)), 3.15 (d, J = 6.9 Hz, 2H, S−CH_2−CH).

Synthesis of the Dopamine-Based Chain Transfer Agent (Dopa-CTA). Suc-CTA (5 g, 14.3 mmol) and dopamine hydrochloride (3 g, 15,8 mmol) were stirred in methanol (150 mL) with triethylamine (2.4 mL, 17.2 mmol) at room temperature under a nitrogen atmosphere, in the dark, for 48 h. The solvent was evaporated and diethyl ether (50 mL) was added. The organic phase was washed with water (3 × 100 mL) and dried over $MgSO_4$. The solvent was evaporated and the product was precipitated into hexane to create a light orange solid in 65% yield.

^{1}H NMR (300 MHz, $CDCl_3$), δ (ppm from TMS): 0.94 (d, J = 6.7 Hz, 6H, CH-(CH_3)$_2$), 1.58 (s, 6H, C(CH_3)$_2$), 1.89 (m, 1H, CH_2−CH-(CH_3)$_2$), 2.6 (t, J = 7.0 Hz, 2H, CH_2−CH_2−Aryl), 3.10 (d, J = 6.9 Hz, 2H, S−CH_2−CH), 3.37 (q, 2H, NH−CH_2−CH_2), 6.1 (br, 1H, Aryl−OH), 6.47 (dd, 1H Aryl−H_a), 6.62 (t, 1H, CO−NH−CH_2), 6.73 (d, 1H, Aryl−H_b), 6.65 (s, 1H, Aryl−H_c), 7.15 (br, 1H, Aryl−OH).

^{13}C NMR (75 MHz, $CDCl_3$): 22.1 (C(CH_3)$_2$), 25.8 (CH(CH_3)$_2$), 27.8 (CH(CH_3)$_2$), 34.5 (CH_2−CH_2−NH), 41.8 (CH_2−CH_2−NH), 45.5 (S−CH_2−CH), 57.0 (C(CH_3)$_2$), 115.2 (C_{aryl}−H(*o*-*OH*), 115.4 (C_{aryl}−H(*o*-*OH*)), 120.7(C_{aryl}−H(*p*-*OH*)), 130.6 ($C^{IV}{}_{aryl}$−CH_2), 142.9 ($C^{IV}{}_{aryl}$−OH), 144.2 ($C^{IV}{}_{aryl}$−OH), 173.5 (C═O), 220.1 (C═S).

FT-IR (cm^{-1}, KBr): 3360 and 3475 (N−H), 3037 (═C−H), 2952 (−C−H), 1651 (C═O), 1611 (N−H), 1444 (C−N), 1057 (C═S).

Anal. Calcd (%) for $C_{17}H_{25}NO_3S_3$: C, 52.68; H, 6.51; N, 3.61. Found: C, 52.86; H, 6.51; N, 3.71.

Synthesis of the Phenyl-Based Chain Transfer Agent (Phi-CTA). A solution of benzyl alcohol (1.57 g, 14.4 mmol) in dichloromethane (50 mL) was added slowly, at room temperature and under a nitrogen atmosphere, to a solution containing 2-(1-isobutyl) sulfanylthiocarbonylsulfanyl-2-methylpropionic acid (CTA, 3.0 g, 12 mmol), DCC (3.0 g, 14.5 mmol) and DMAP (1.5 g, 12 mmol) in dichloromethane (200 mL). The reaction was stirred overnight. After filtration, the solution was washed with distilled water (3 × 50 mL) and dried over $MgSO_4$. The product was purified by column chromatography (SiO_2: dichloromethane/petroleum ether 1: 1). The product was obtained as an orange oil in 60% yield.

^{1}H NMR (300 MHz, $CDCl_3$), δ (ppm from TMS): 0.92 (d, J = 6.7 Hz, 6H, CH−(CH_3)$_2$), 1.64 (s, 6H C(CH_3)$_2$), 1.88 (m, 1H, CH_2−CH−(CH_3)$_2$), 3.10 (d, J = 6.9 Hz, 2H, S−CH_2−CH), 5.05 (s, 2H, C_6H_5−CH_2−O), 7.26 (m, 5H, C_6H_5−CH_2).

^{13}C NMR (75 MHz, $CDCl_3$): 22.1 (C(CH_3)$_2$), 25.4 (CH(CH_3)$_2$), 27.8 (CH(CH_3)$_2$), 45.2 (S−CH_2−CH), 56.0 (C(CH_3)$_2$), 67.7 (C_6H_5−CH_2−O), 128.1, 128.5 (C_{aryl}−H),), 135.6 ($C^{IV}{}_{aryl}$−CH_2), 172.9 (C═O), 221.5 (C═S).

FT-IR (cm^{-1}, KBr): 3037 (═C−H), 2959 and 2869 (C−H), 1725 (C═O), 1498 and 1463 (C═C), 1258 (C−O), 1061 (C═S).

Typical Procedure for RAFT-Mediated Polymerizations. In a Schlenk tube were added monomer (styrene, *t*BA, or NIPAM), AIBN, and the chain transfer agent (CTA) in toluene (3.5 g) or DMF (0.5 g). The mixture was deoxygenated by nitrogen bubbling for 30 min. The mixture was then heated to the desired temperature (80 °C for styrene and tBA and 75 °C for NIPAM). Samples were periodically withdrawn to measure both the monomer conversion by ^{1}H NMR and polymer characteristics by size exclusion chromatography. The final polymer was recovered by precipitation of the mixture in ethanol (Polystyrene and P*t*BA) or diethyl ether (PNIPAM). After filtration, the product was dried under vacuum until achieving a constant weight.

Preparation of Functionalized Titanium Surfaces ("Graft to" Method). Titanium plates (o.d. = 1.5 cm) were first treated with an acidic oxidizing solution of concentrated sulfuric acid and hydrogen peroxide H_2SO_4/H_2O_2 (1:1) for 2 min to generate the corresponding hydroxylated titanium dioxide surface. Titanium plates were thoroughly rinsed with water, acetone, and ethanol, and dried under nitrogen before functionalization. The pretreated titanium surfaces were then soaked

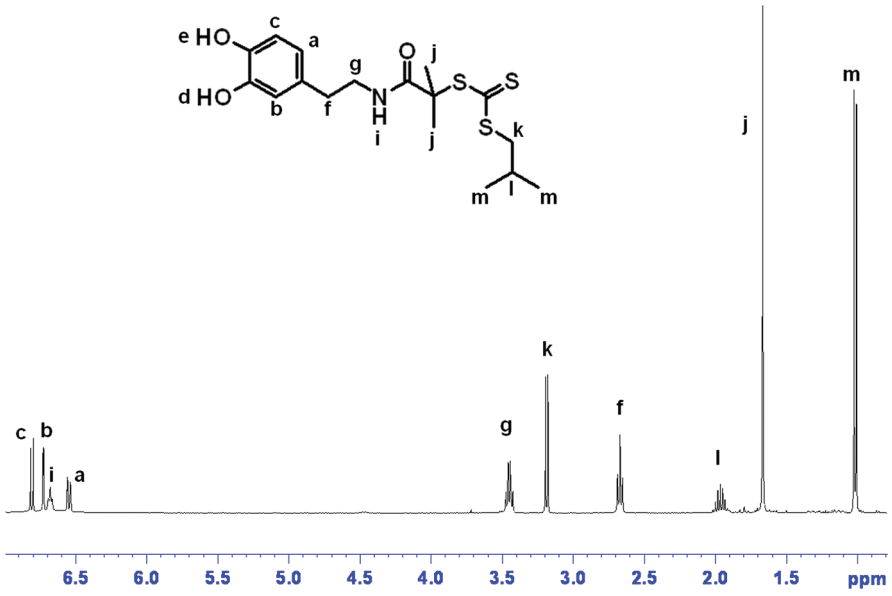

Figure 1. ^{1}H NMR spectrum of Dopa-CTA (300 MHz, $CDCl_3$).

Table 1. Results for the Polymerizations of Styrene, tBA, and NIPAM Performed in the Presence of Dopa-CTA and Azobis(isobutyronitrile) (AIBN) as Initiator[a]

monomer	$[M]_0/[CTA]_0/[AIBN]_0$	time (min)	convn[b] (%)	$M_{n,th}$ (g mol^{-1})	$M_{n,SEC}$[c] (g mol^{-1})	PDI[d]
Styrene	150/1/0.3	60	4.8	890	1900	1.03
		180	14.2	1860	2900	1.05
		240	16.5	2110	2920	1.05
		300	19.7	2430	3130	1.05
tBA	100/1/0.05	60	5.3	1900	1700	1.13
		120	31.4	4400	4800	1.11
		180	46.6	6350	6600	1.11
		240	55.4	7470	7700	1.12
NIPAM	100/1/0.1	120	22.8	2960	2800	1.07
		180	54.7	6570	5100	1.09
		270	73.4	8690	6400	1.11
		330	78.9	9310	7500	1.11

[a] Reaction conditions: T = 75 °C for NIPAM and *t*BA, 80 °C for styrene; solvent, DMF for NIPAM and toluene for *t*BA and styrene. [b] Determined by ^{1}H NMR. [c] Number-average molar mass, $M_{n,SEC}$ determined by size exclusion chromatography using PS standards for the synthesized polystyrene, P(tBA) and for PNIPAM. [d] Polydispersity index determined by SEC.

in a solution containing 0.5 mM of polymer in water for Dopa-PNIPAM, acetonitrile for Dopa-P*t*BA, and THF/water mixture (9:1) for Dopa-PS. Samples were soaked overnight, washed with the solvent used for the grafting and, finally, dried under nitrogen to obtain the functionalized titanium surface.

RESULTS AND DISCUSSION

Synthesis of the Dopamine-Functionalized Chain Transfer Agent. A new RAFT agent was specially designed to entail the catechol fragment required for the titanium grafting (Scheme 1). The RAFT agent Dopa-CTA was conveniently prepared from the coupling reaction of the *N*-hydroxysuccinimide (NHS) activated ester of the trithiocarbonate 2-(1-isobutyl)sulfanylthiocarbonylsulfanyl-2-methyl propionic acid (CTA) and the commercially available dopamine hydrochloride. The structure of the Dopa-CTA was confirmed by ^{1}H NMR, ^{13}C NMR, UV−vis and FTIR spectroscopy. ^{1}H NMR spectrum of Dopa-CTA recorded in $CDCl_3$ at 25 °C revealed the presence of the characteristic signals of the catechol unit (6 to 7 ppm) and those bearing by the isobutylsulfanylthiocarbonylsulfanyl [$(CH_3)_2CH-CH_2-S-(C=S)-S-$] moiety (Figure 1). Furthermore, the ^{13}C spectrum (see Supporting Information) clearly displayed chemical shifts at 173.4 and 220.0 ppm ascribed to the amide carbonyl group and the thiocarbonyl fragment of Dopa-CTA, respectively. Finally, the structure of Dopa-CTA was further confirmed by UV−vis (10^{-4} mM in MeOH, see Supporting Information, Figure SI2) and IR (see Supporting Information, Figure SI3) investigations, as a strong UV absorption at around 310 nm and an IR characteristic peak at 1057 cm^{-1} were observed, which can be assigned to the C=S bond.[38]

RAFT Polymerizations using Dopa-CTA. First, the ability of Dopa-CTA to promote RAFT polymerizations of different monomers (NIPAM, *t*BA, Styrene) was tested. A series of

dx.doi.org/10.1021/ma200853w |*Macromolecules* 2011, 44, 5883–5892

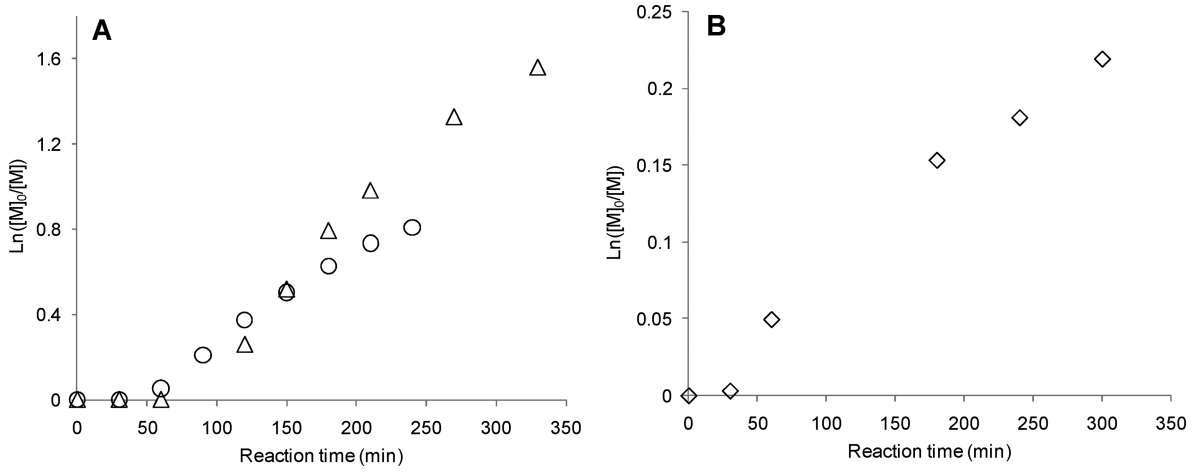

Figure 2. Semilogarithmic kinetic curves for RAFT polymerizations: (A) NIPAM (Δ) and tBA (○); (B) styrene (◇). For reaction conditions, refer to Table 1.

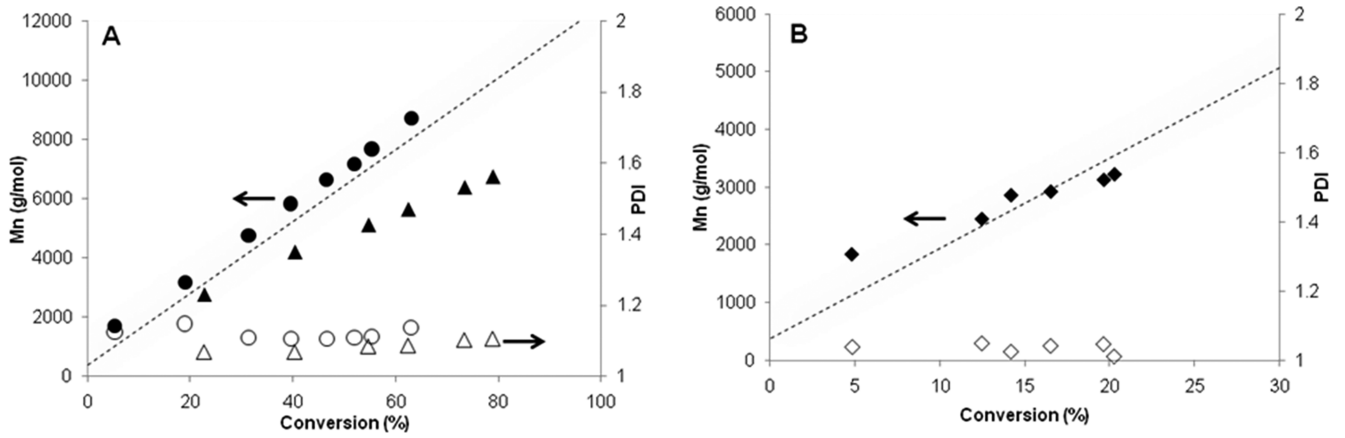

Figure 3. Dependence of the molar masses (filled symbols) and the PDI (open symbols) of obtained polymers on monomer conversion during the RAFT polymerizations of NIPAM (A, Δ▲), *t*BA(A, ○●) and styrene (B, ◇◆). The straight lines correspond to the theoretically expected M_n.

polymerizations initiated by AIBN in the presence of Dopa-CTA were conducted in DMF at 75 °C for *N*-isopropylacrylamide (NIPAM), in toluene at 75 °C for *tert*-butyl acrylate (*t*BA) and in toluene at 80 °C for styrene.

The polymerization conditions and results of RAFT polymerizations of NIPAM, *t*BA and styrene are summarized in Table 1. The $\ln([M]_0/[M])$ vs time plots (Figure 2) for RAFT polymerizations of various monomers is reported. After a typical induction period,[39] the first-order kinetic plot was linear in all cases indicating that the concentration of active species was constant, which is essential in controlled radical polymerizations. Using this trithiocarbonate as the CTA agent, it appears that the polymerization rate was higher for NIPAM polymerization than *t*BA polymerization, the polymerization rate for styrene polymerization being the lowest, consistent with our previous study.[40]

Figure 3 shows the evolution of the molecular masses and polydispersity indices of the resulting polymers as a function of monomer conversion. In all cases, molecular weights of the PNIPAM, P(*t*BA) and PS increased linearly and the polydispersity indices remained relatively low as the monomer conversion progressed. Moreover, all of the synthesized polymers showed rather symmetrical and narrow SEC traces (see Supporting Information). Both kinetic plots and SEC results proved that Dopa-CTA allowed for an excellent control of the polymerization of different kinds of monomers.

Characterizations of Polymers. The structure of synthesized polymers was elucidated by ^{1}H NMR. For instance, as shown in Figure 4 for dopamine-terminated PNIPAM, the presence of the catechol unit in polymers was indicated by its ^{1}H NMR typical resonances between 6.5 and 6.75 ppm (for H_f, H_g and H_h, see enlarged part, Figure 4), and at 2.5 ppm for the benzylic protons H_i. Moreover, ^{1}H NMR spectra also displayed resonances around 3.2 ppm belonging to the methylene protons H_k of the isobutylsulfanylthiocarbonyl sulfanyl moiety, providing further evidence of the ability of Dopa-CTA to act as the CTA in RAFT polymerizations. By taking into account the integration of one proton from the Dopa-CTA (H_g, H_h or H_f, Figure 4) and one proton from the repeating unit NIPAM (H_c, Figure 4), the molecular weight of the polymer could be calculated ($M_{n,NMR}$ = 12 500 g·mol^{-1}).

The UV−vis spectroscopy confirmed the presence of the terminal trithiocarbonate group on the dopamine end-functionalized polymers. Indeed, the UV−vis spectra of dopamine end-functionalized polymers (Figure 5) exhibited a wide characteristic

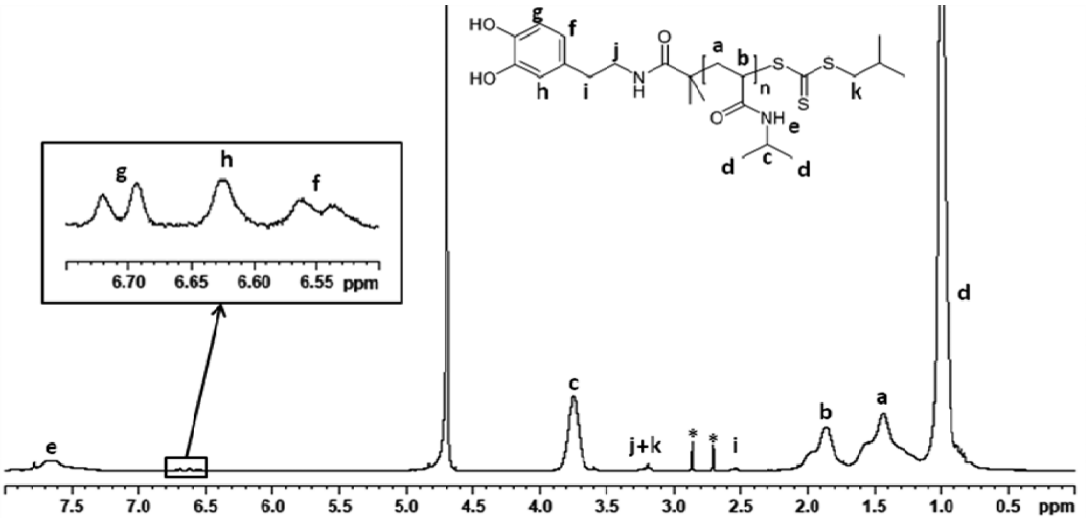

Figure 4. ^{1}H NMR spectrum of dopamine-terminated PNIPAM (300 MHz, D_2O). Peaks marked with asterix correspond to remaining solvent.

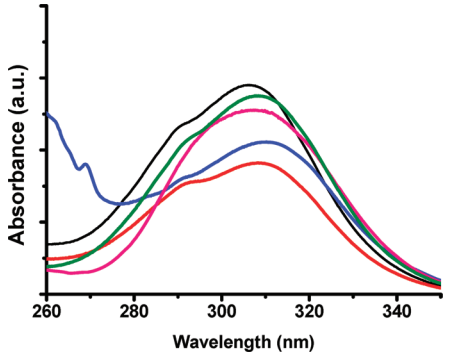

Figure 5. UV−vis spectrum of dopamine end-functionalized P*t*BA (−), PNIPAM (red line), PS (blue line), Dopa-CTA (green line) (ε = 13460 L.mol^{-1}.cm^{-1}, λ_{max} = 308 nm) and Phi-PNIPAM (violet line).

absorption band around 310 nm as observed for the Dopa-CTA (green line) and Phi-PNIPAM (violet line) (which does not incorporate a catechol unit), corresponding to the chromophoric C═S bond of the CTA group.

Finally, the presence of catechol fragments in the polymer chains was further evidenced by recording cyclic voltamograms (CV) in acetonitrile (or acetonitrile/dichloromethane 1:1 in the case of Dopa-PS) using Bu_4NPF_6 (0.05 M) as the supporting electrolyte (Figure 6). Indeed, for all dopamine end-functionalized polymers and as observed for the Dopa-CTA derivative, CV gave rise to the irreversible two-electron oxidation wave around 1.1 V vs Ag/AgCl, corresponding to the two-step oxidation of the catechol unit.[31] Dopa-based polymers showed no significant shifts in the position of the oxidation wave, suggesting that the polymer chain does not affect the redox properties of the Dopamine unit. An interesting feature of the CV of the Dopa-PNIPAM derivative is the difference in the shape of the peak corresponding to the formation of oxidized species of the dopamine fragment compared to other polymer systems, indicating that the PNIPAM backbone may interact with the electroactive unit.[40]

Immobilization of Dopamine End-Functionalized Polymers on a Titanium Surface. Prior to the immobilization, the titanium surface was pretreated with an acidic oxidizing solution of concentrated sulfuric acid and hydrogen peroxide (H_2SO_4/H_2O_2 1:1) to generate the corresponding hydroxylated titanium

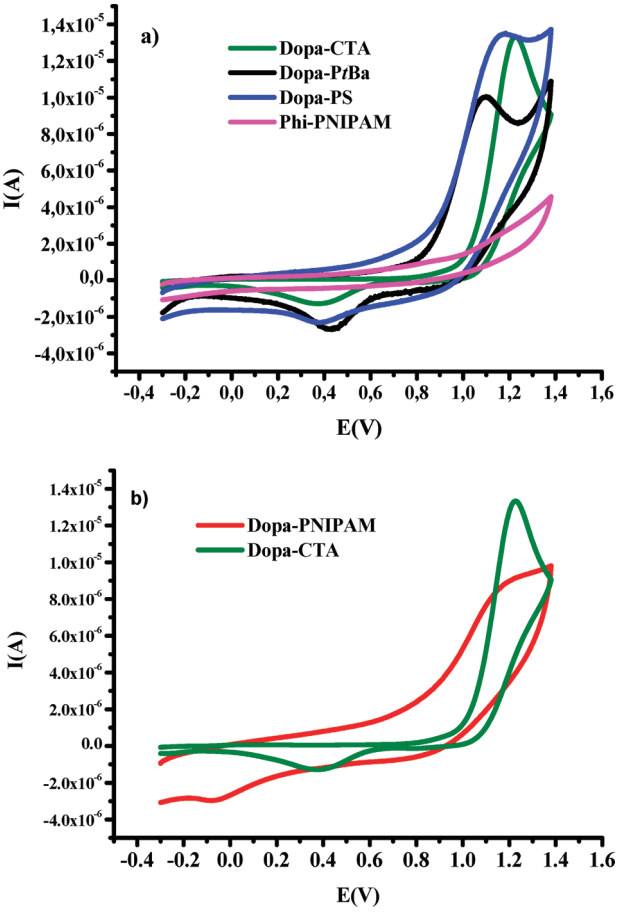

Figure 6. Cyclic voltamograms of (a) Dopa-CTA, Dopa-P*t*BA, and Phi-PNIPAM in acetonitrile and Dopa-PS in acetonitrile/dichloromethane (1:1, v:v) and (b) Dopa-CTA and Dopa-PNIPAM in acetonitrile. CV were recorded at $C = 10^{-3}$ M in the presence of Bu_4NPF_6 (0.05 M). Platinum working electrode; Ag/AgCl reference electrode. Scan rate of 50 mV s^{-1}.

Scheme 2. Illustration of the Functionalization of Titanium Surfaces with Dopamine End-Functionalized Brushes Polymers Prepared from the Dopa-CTA RAFT Agent

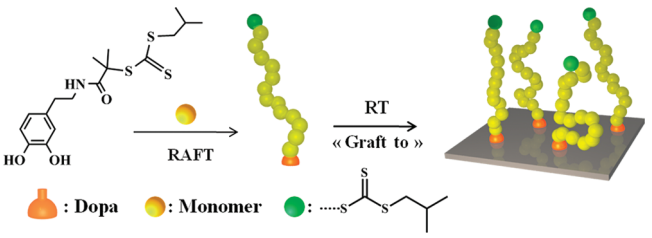

Table 2. XPS Atomic Ratios and Contact Angle Measurements of Polymers Grafted onto Titanium Surfaces

	XPS atomic concentration (%)				
samples	C 1s	O 1s	Ti 2p	N 1s	static water contact angle (deg)
Ti	30.0	37.6	19.3	0.9	23 ± 3
Dopa-PNIPAM	46.9	28.9	10.4	4.14	74 ± 2
Dopa-P*t*BA	64.6	21.2	6.27	0.6	90 ± 2
Dopa-PS	54.6	26.32	8.40	1.03	110 ± 2

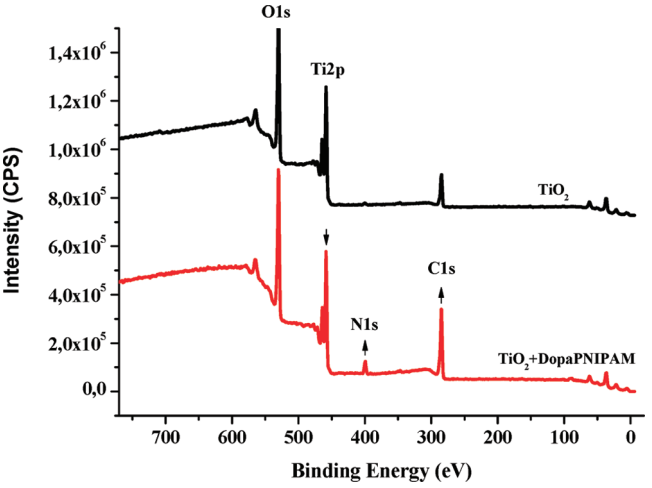

Figure 7. Partial XPS survey spectra of titanium surface before and after grafting of the dopamine end-functionalized PNIPAM.

dioxide surface[31] which allows the bidentate catechol ligand to strongly adhere to the TiO_2 surface. The pretreated titanium surface was then soaked in a solution containing 0.5 mM of dopamine end-functionalized polymer overnight, resulting in (after washing) the polymer functionalized titanium surface ("grafting to" method, Scheme 2).

XPS Investigations. Successful immobilization of the polymers on the titanium surface was first investigated by XPS. Chemical compositions of end-functionalized grafted polymer and unmodified titanium surfaces are summarized in Table 2. As expected, the XPS-determined elemental composition of the unmodified titanium surface showed the presence of titanium and oxygen components. Carbon, nitrogen, and cationic species

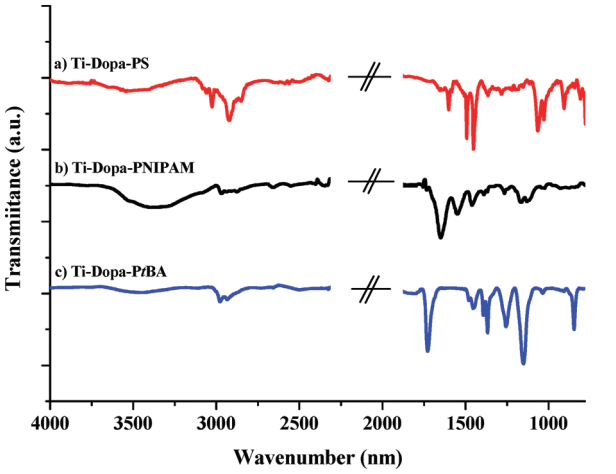

Figure 8. IR-ATR Spectra of titanium surfaces functionalized with (a) Dopa-PS, (b) Dopa-PNIPAM, and (c) Dopa-P*t*BA. The 1900−2300 cm^{-1} region corresponding to the Zn−Se crystal absorption band is omitted for more clearness.

were also detected, which are likely due to contamination arising from the polishing and cleaning of the titanium samples.[1,41,42]

After polymer grafting, an increase in the carbon signal and a decrease in the titanium and oxygen ratios were observed in the XPS survey (Figure 7), which are consistent with the immobilization of polymers on the surface. Furthermore, in the case of titanium surfaces modified with Dopa-PNIPAM, an increase of the nitrogen ratio was observed as evidenced in the XPS survey spectra (Figure 7). Finally, a film thickness of 3−5 nm could be estimated from the attenuation of the Ti signal.[43]

Contact Angle Measurements. The impact of polymer grafting on the titanium surface wettability was investigated with static contact angle measurements (Table 2). The unmodified titanium surface exhibited a low contact angle of 23 ± 3° consistent with the presence of hydrophilic hydroxyl Ti−OH groups on the titanium surface subsequent to the oxidation step. Treatment of this surface with Dopa-P*t*BA, Dopa-PS, and Dopa-PNIPAM induced, in both cases, a dramatic increase of the contact angle. The measured contact angles were 90 ± 2°, 110 ± 2°, and 74 ± 2° with Dopa-P*t*BA, Dopa-PS, and Dopa-PNIPAM, respectively, which agreed with the reported values.[44−46]

IR-ATR. The grafting of dopamine end-functionalized polymers onto the titanium surface was further characterized by infrared spectroscopy using the attenuated total reflectance (ATR) technique. The IR-ATR spectrum of the titanium sample functionalized with Dopa-PS (Figure 8a) exhibited the characteristic absorption bands at 3025 cm^{-1} and at 1450, 1490, and 1600 cm^{-1} assigned to C−H aromatic and C═C aromatic stretching of the polystyrene backbone, respectively.[47]

The grafting of the Dopa-PNIPAM polymer onto the titanium surface was revealed in the IR spectrum (Figure 8b) by the appearance of N−H and C═O stretching bands at 3350 and 1650 cm^{-1}, respectively. An additional peak at 1546 cm^{-1} assigned to the N−H bending further indicated the presence of the amide group in the polymer layer.

Finally, the functionalization of the titanium surface with Dopa-P*t*BA was evidenced by IR-ATR by the appearance of the characteristic absorption band of the carbonyl group at 1725 cm^{-1}.

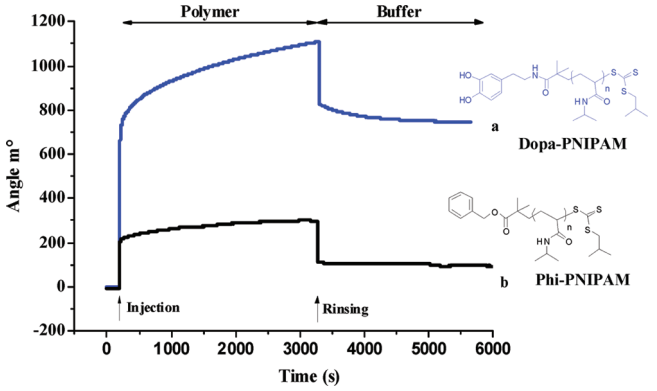

Figure 9. SPR sensograms recorded on the titanium surface during the injection of (a) Dopa-PNIPAM (M_n = 12 500 g·mol^{-1}, PDI = 1.10) and (b) Phi-PNIPAM (M_n = 9500 g·mol^{-1}, PDI = 1.10); [polymer] = 0.25 mM in water; buffer = water, T = 20 °C.

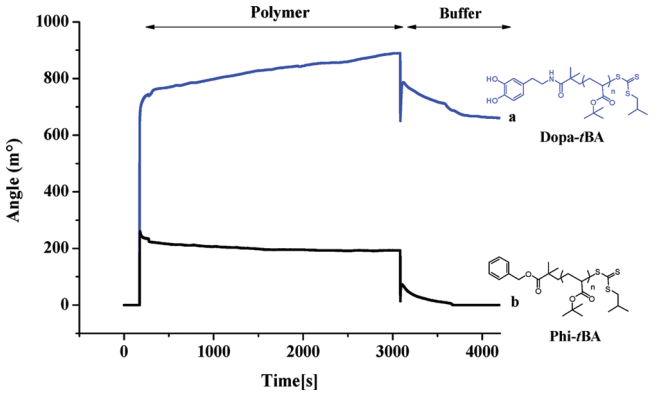

Figure 10. SPR sensograms recorded on the titanium surface during injection of (a) Dopa-P*t*BA (M_n = 9000 g·mol^{-1}, PDI = 1.12) and (b) Phi-P*t*BA (M_n = 10 000 g·mol^{-1}, PDI = 1.14); [polymer] = 1 mM in acetonitrile; buffer = acetonitrile.

Surface Plasmon Resonance. The ability of dopamine end-functionalized PNIPAM and *tert*-butyl polymers to coordinate with a titanium surface was also investigated by surface plasmon resonance (SPR) spectroscopy in water and acetonitrile, respectively.[48] SPR is a label-free optical technique which is sensitive to the changes in refractive index and thickness in the close vicinity of the metal layer.[49,50] Here, we have exploited this technique to (i) study the binding events between polymers (Dopa-PNIPAM and Dopa-P*t*BA) and the titanium surface, (ii) investigate the role played by the catechol anchor in the immobilization process, and (iii) get quantitative information such as surface coverage.

As illustrated in Figure 9a, sensorgrams obtained for the dopamine end-functionalized PNIPAM ($M_{n,NMR}$ = 12500 g·mol^{-1}, PDI = 1.10), recorded below its LCST (≈ 32 °C, see Supporting Information), successively exhibited a dramatic shift of the SPR angle after injection and then a progressive increase of reflectance, which is indicative of adsorption and the formation of an organic layer on the titanium surface.

Next, rinsing the SPR cell with water caused a small decrease of the resonance angle, suggesting that no significant physisorption occurred. Moreover, subsequent extensive rinsing had no evidential impact on the resonance angle, implying that a stable polymer brush was formed.

SPR experiments were also performed on the Dopa-P*t*BA (M_n = 9000 g·mol^{-1}, PDI = 1.12) (Figure 10) in acetonitrile and showed trends similar to those observed for Dopa-PNIPAM, indicating that dopamine end-functionalized polymers can also bind with the titanium surface in the nonaqueous phase.

In order to investigate the role played by the catechol anchor, we have studied the ability of Phi-PNIPAM (M_n = 9500 g·mol^{-1} PDI = 1.12) and Phi-P*t*BA (M_n = 10000 g·mol^{-1} PDI = 1.14), which do not bear a catechol fragment, to interact with the titanium surface by SPR in aqueous media and acetonitrile, respectively. As shown in Figures 9b and 10b, in both cases rinsing almost restored the SPR signal to the baseline, suggesting that no coordination occurred and thereby indicating the important role of the catechol unit in the formation of stable brush polymers.

Finally, the amount of bonded Dopa-PNIPAM and Dopa-P*t*BA on the Ti sensor surface was calculated from the difference between SPR signal of samples after the immobilization procedure was finished and the SPR signal of the solvent (Table 3).

By using the De Feijter equation[51] (see Supporting Information), the surface coverage Γ of the grafted polymers on the sensor surface was calculated to be 4.4 × 10^{12} and 12.4 × 10^{12} molecules/cm^2 for Dopa-PNIPAM and Dopa-P*t*BA, respectively. These grafting densities are lower than those expected for self-assembled monolayers (10^{14} molecules/cm^2).[52] Thus, taking also into account the thicknesses (3−4 nm) estimated by

Table 3. Estimation of Surface Coverage Γ from SPR Investigations

	SPR Surface Coverage			
polymers	M_n (g mol^{-1})	PDI	C (mM)	Γ (molecules/cm^2)
Dopa-PNIPAM	12500	1.10	0.25	4.4 × 10^{12}
Dopa-*t*BA	9000	1.12	1	12.4 × 10^{12}

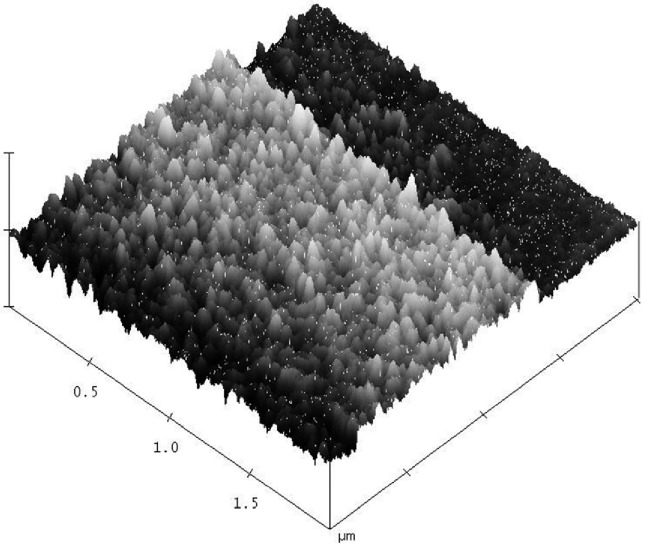

Figure 11. AFM image of the titanium surface modified with dopamine end-functionalized PNIPAM. The AFM image is a topographical image with an image size of 2 × 2 μm.

XPS, these SPR results suggest that polymers are highly canted on the surface or are in a mushroom formation.[53,54]

Atomic Force Microscopy. Finally, atomic force microscopy was used to analyze the surface topography of the titanium film deposed from Dopa-PNIPAM (M_n = 21 000 g·mol^{-1}, PDI = 1.15). For this purpose, a titanium sample was half immersed in a 0.5 mM solution of Dopa-PNIPAM in water overnight. After rinsing with water and drying, AFM images were recorded in tapping mode. The resulting AFM image (Figure 11) clearly indicates the grafting of the end-functionalized polymer onto the titanium surface, as a neat step between the modified and unmodified surface is evidenced. Visual inspection suggests a near-homogeneous grafted layer having a thickness of around 4−5 nm, in accordance with XPS results.

CONCLUSIONS

In conclusion, well-defined dopamine end-functionalized polymers have been prepared via RAFT polymerization. A new RAFT agent including a catechol unit fragment was designed and used to mediate homopolymerizations of *tert*-butyl acrylate, *N*-isopropylacrylamide, and styrene. Characteristic features of controlled polymerizations were observed and a range of polymers with controlled molar mass and narrow molar mass distributions were prepared. The grafting of dopamine end-functionalized polymers was monitored in real time by SPR and confirmed by XPS, ATR, contact angle, and AFM investigations. Our future work will focus on the preparation of well-defined dopamine end-functionalized polymers incorporating long side-chain stimulable and/or bioactive units and on their subsequent immobilization on titanium surfaces, with the goal of creating smart biomaterials. These works will be reported in due course.

ASSOCIATED CONTENT

Supporting Information. Characterization spectra of Dopa-CTA and Phenyl-CTA. and GPC traces of polymers. This material is available free of charge via the Internet at http://pubs.acs.org

AUTHOR INFORMATION

Corresponding Author

*E-mail: patrice.woisel@ensc-lille.fr.

ACKNOWLEDGMENT

The authors would like to thank CNRS, the Region Nord/Pas-de-Calais and the European FEDER program for funding to Surface Plasmon Resonance (SPR) apparatus at UMET. We thank Aurélie Malfait for the GPC analysis and Catherine MELIET for her assistance with the elemental analyses. The Region Nord Pas-de-Calais and PRIM SP are thanked for funding of the ELEMENTAR, vario MICRO equipment.

REFERENCES

(1) Brunette, D.; Tengvall, P.; Textor, M., *Titanium in Medicine: Material Science, Surface Science, Engineering, Biological Responses and Medical Applications (Engineering Materials)*; Springer: Berlin, 2001.
(2) Niinomi, M. *Mater. Sci. Eng., A* **1998**, *243*, 231–236.
(3) Thomas, R. *Geothermics* **2003**, *32*, 679–687.
(4) Li, L.; Hu, W.; Chi, L.; Fuchs, H. *J. Phys. Chem. B* **2010**, *114*, 5315–5319.
(5) Brunette, D.; Wieland, M.; Tosatti, S.; Textor, M. Use of Molecular Assembly Techniques for Tailoring Chemical Properties of Smooth and Rough Titanium Surfaces. In *Bio-Implant Interface*; CRC Press: Boca Raton, FL, 2003.
(6) Xiong, L.; Liang, H.; Wang, R.; Chen, L. *J. Polym. Res.* **2010**, 1–5.
(7) Meuer, S.; Fischer, K.; Mey, I.; Janshoff, A.; Schmidt, M.; Zentel, R. *Macromolecules* **2008**, *41*, 7946–7952.
(8) Zoulalian, V.; Monge, S.; Zürcher, S.; Textor, M.; Robin, J. J.; Tosatti, S. *J. Phys. Chem. B* **2006**, *110*, 25603–25605.
(9) Zoulalian, V.; Zürcher, S.; Tosatti, S.; Textor, M.; Monge, S.; Robin, J.-J. *Langmuir* **2009**, *26*, 74–82.
(10) Porté-Durrieu, M. C.; Guillemot, F.; Pallu, S.; Labrugère, C.; Brouillaud, B.; Bareille, R.; Amédée, J.; Barthe, N.; Dard, M.; Baquey, C. *Biomaterials* **2004**, *25*, 4837–4846.
(11) Barbey, R. l.; Lavanant, L.; Paripovic, D.; Schüwer, N.; Sugnaux, C.; Tugulu, S.; Klok, H.-A. *Chem. Rev.* **2009**, *109*, 5437–5527.
(12) Ma, H.; Wells, M.; Beebe, T. P.; Chilkoti, A. *Adv. Funct. Mater.* **2006**, *16*, 640–648.
(13) Ma, H.; Li, D.; Sheng, X.; Zhao, B.; Chilkoti, A. *Langmuir* **2006**, *22*, 3751–3756.
(14) Bünsow, J.; Kelby, T. S.; Huck, W. T. S. *Acc. Chem. Res.* **2009**, *43*, 466–474.
(15) Liu, X.; Ye, Q.; Yu, B.; Liang, Y.; Liu, W.; Zhou, F. *Langmuir* **2010**, *26*, 12377–12382.
(16) Nagase, K.; Kobayashi, J.; Okano, T. *J. R. Soc. Interface* **2009**, *6*, S293–S309.
(17) Minko, S. Grafting on Solid Surfaces: "Grafting to" and "Grafting from" Methods. In *Polymer Surfaces and Interfaces*, Stamm, M., Ed.; Springer: Berlin and Heidelberg, Germany, 2008; pp 215−234.
(18) Ye, Q.; Wang, X.; Li, S.; Zhou, F. *Macromolecules* **2010**, *43*, 5554–5560.
(19) Raynor, J. E.; Petrie, T. A.; Fears, K. P.; Latour, R. A.; García, A. s. J.; Collard, D. M. *Biomacromolecules* **2009**, *10*, 748–755.
(20) Raynor, J. E.; Petrie, T. A.; García, A. J.; Collard, D. M. *Adv. Mater.* **2007**, *19*, 1724–1728.
(21) Matyjaszewski, K.; Xia, J. *Chem. Rev.* **2001**, *101*, 2921–2990.
(22) Gao, C.; Li, G.; Xue, H.; Yang, W.; Zhang, F.; Jiang, S. *Biomaterials* **2010**, *31*, 1486–1492.
(23) Rowe-Konopacki, M. D.; Boyes, S. G. *Macromolecules* **2007**, *40*, 879–888.
(24) Pissuwan, D.; Boyer, C.; Gunasekaran, K.; Davis, T. P.; Bulmus, V. *Biomacromolecules* **2010**, *11*, 412–420.
(25) Hojjati, B.; Sui, R.; Charpentier, P. A. *Polymer* **2007**, *48*, 5850–5858.
(26) Fan, X.; Lin, L.; Dalsin, J. L.; Messersmith, P. B. *J. Am. Chem. Soc.* **2005**, *127*, 15843–15847.
(27) Statz, A. R.; Meagher, R. J.; Barron, A. E.; Messersmith, P. B. *J. Am. Chem. Soc.* **2005**, *127*, 7972–7973.
(28) Dalsin, J. L.; Hu, B.-H.; Lee, B. P.; Messersmith, P. B. *J. Am. Chem. Soc.* **2003**, *125*, 4253–4258.
(29) Ye, Q.; Wang, X.; Hu, H.; Wang, D.; Li, S.; Zhou, F. *J. Phys. Chem. C* **2009**, *113*, 7677–7683.
(30) Liu, J.; Yang, W.; Zareie, H. M.; Gooding, J. J.; Davis, T. P. *Macromolecules* **2009**, *42*, 2931–2939.
(31) Watson, M. A.; Lyskawa, J.; Zobrist, C.; Fournier, D.; Jimenez, M.; Traisnel, M.; Gengembre, L.; Woisel, P. *Langmuir* **2010**, *26*, 15920–15924.
(32) Goldmann, A. S.; Schödel, C.; Walther, A.; Yuan, J.; Loos, K.; Müller, A. H. E. *Macromol. Rapid Commun.* **2010**, *31*, 1608–1615.
(33) Song, H. M.; Ye, P. D.; Ivanisevic, A. *Langmuir* **2007**, *23*, 9472–9480.
(34) Dalsin, J. L.; Lin, L.; Tosatti, S.; Vörös, J.; Textor, M.; Messersmith, P. B. *Langmuir* **2004**, *21*, 640–646.
(35) Wach, J.-Y.; Malisova, B.; Bonazzi, S.; Tosatti, S.; Textor, M.; Zürcher, S.; Gademann, K. *Chem.—Eur. J.* **2008**, *14*, 10579–10584.
(36) Fan, X.; Lin, L.; Messersmith, P. B. *Compos. Sci. Technol.* **2006**, *66*, 1198–1204.

(37) Qiu, X.-P.; Tanaka, F.; Winnik, F. M. *Macromolecules* **2007**, *40*, 7069–7071.
(38) Ran, R.; Yu, Y.; Wan, T. *J. Appl. Polym. Sci.* **2007**, *105*, 398–404.
(39) Moad, G.; Barner-Kowollik, C., *The Mechanism and Kinetics of the RAFT Process: Overview, Rates, Stabilities, Side Reactions, Product Spectrum and Outstanding Challenges*; Wiley-VCH Verlag GmbH & Co. KGaA: Weinheim, Germany, 2008; pp 51−104.
(40) Bigot, J.; Charleux, B.; Cooke, G.; Delattre, F.; Fournier, D.; Lyskawa, J.; Stoffelbach, F.; Woisel, P. *Macromolecules* **2010**, *43*, 82.
(41) Viornery, C.; Chevolot, Y.; Léonard, D.; Aronsson, B.-O.; Péchy, P.; Mathieu, H. J.; Descouts, P.; Grätzel, M. *Langmuir* **2002**, *18*, 2582–2589.
(42) Nanci, A.; Wuest, J. D.; Peru, L.; Brunet, P.; Sharma, V.; Zalzal, S.; McKee, M. D. *J. Biomed. Mater. Res* **1998**, *40*, 324–335.
(43) Laforgue, A.; Addou, T.; Bélanger, D. *Langmuir* **2005**, *21*, 6855–6865.
(44) Walters, K. B.; Hirt, D. E. *Polymer* **2006**, *47*, 6567–6574.
(45) Li, Y.; Pham, J. Q.; Johnston, K. P.; Green, P. F. *Langmuir* **2007**, *23*, 9785–9793.
(46) Gilcreest, V. P.; Carroll, W. M.; Rochev, Y. A.; Blute, I.; Dawson, K. A.; Gorelov, A. V. *Langmuir* **2004**, *20*, 10138–10145.
(47) Pei, Z.; Busenlehner, L.; Worley, S. D.; Tang, Y.; Curtis, C. W. *J. Phys. Chem. B* **1997**, *101*, 10450–10454.
(48) The immobilization of dopamine end-functionalized PS was not studied by SPR due to its poor solubility in employed solvents
(49) Homola, J.; Yee, S. S.; Gauglitz, G. *Sens. Actuators B: Chem.* **1999**, *54*, 3–15.
(50) Chang, Y.; Chu, W.-L.; Chen, W.-Y.; Zheng, J.; Liu, L.; Ruaan, R.-C.; Higuchi, A. *J. Biomed. Mater. Res., Part A* **2010**, *93A*, 400–408.
(51) De Feijter, J. A.; Benjamins, J.; Veer, F. A. *Biopolymers* **1978**, *17*, 1759–1772.
(52) Zareie, H. M.; Boyer, C.; Bulmus, V.; Nateghi, E.; Davis, T. P. *ACS Nano* **2008**, *2*, 757–765.
(53) Wu, T.; Efimenko, K.; Genzer, J. *J. Am. Chem. Soc.* **2002**, *124*, 9394–9395.
(54) Wu, T.; Efimenko, K.; Vlček, P.; Šubr, V.; Genzer, J. *Macromolecules* **2003**, *36*, 2448–2453.